

FBRM and PVM investigations of the double feed semi-batch crystallization of 6-aminopenicillanic acid

Min SU, Lin WANG, Hua SUN, Jingkang WANG (✉)

School of Chemical Engineering and Technology, Tianjin University, Tianjin 300072, China
State Key Laboratory of Chemical Engineering, Tianjin University, Tianjin 300072, China

© Higher Education Press and Springer-Verlag 2009

Abstract 6-Aminopenicillanic acid (6-APA) is a crucial pharmaceutical intermediate in the chemistry of semi-synthetic antibiotics. The focused beam reflectance measurement (FBRM) technology and particle vision measurement (PVM) technology were employed to the processes of online-monitoring of 6-APA crystallization behavior in a double-feeding semi-batch crystallizer. Experiments were carried out with four kinds of double-feeding policies and the results were compared with the traditional single-feeding. Records and analysis of FBRM indicated that the nucleation of double feeding policy was much higher than single policy, and chord length of 6-APA was almost determined and had little change after the nucleation peak. Ostwald ripening process had no significant effect on further growth of 6-APA crystal. PVM images showed that the crystal habit of 6-APA was continuously changed during the crystallization process. The development of (002) face in the final crystal for the five feeding policies were different.

Keywords 6-aminopenicillanic acid, crystallization, double-feeding, FBRM, PVM, crystal habit

1 Introduction

6-Aminopenicillanic acid (6-APA), the nucleus of the original penicillin molecule, is a crucial pharmaceutical intermediate in the chemistry of semi-synthetic antibiotics, from which all penicillin was produced [1].

6-APA has normally been produced by enzymatic hydrolysis of penicillin G, and then the resulting degraded

products may be subjected to an extraction process. Finally, 6-APA is crystallized from the extractive aqueous phase with a flow of acid feeding to the system continuously. This process was also called reactive crystallization [2–4].

The quality of 6-APA is determined by its purity, crystal size distribution, habit, etc, which are strongly influenced by crystallizing conditions, such as local and average supersaturation, solution composition, operating mode of crystallizer, policy of generating supersaturation, temperature, and pressure [5]. Thus, understanding the crystallization behavior of 6-APA under different operational conditions is necessary on account of its industrial importance.

Mwangi and Garside have characterized the habit of 6-APA grown from pure water and solution containing phenoxyacetic acid [6]. Gong has investigated the effect of solution composition, temperature, and supersaturation on the crystal habit modification of 6-APA [7, 8]. Despite much interest on the crystallization of 6-APA, neither particle variation process nor real-time morphology information was investigated in a double-feed semi-batch crystallizer. To design an optimized crystallization process, it is essential to take a real-time observation and analysis to the process.

The focused beam reflectance method (FBRM) and particle vision measurement (PVM) have emerged as widely used techniques in scientific research for real-time characterization of the systems [9–14].

In the present work, such popular techniques were employed to obtain real-time measurements of 6-APA crystallization. With the sensitive techniques of FBRM and PVM, this paper reports an investigation into the real-time crystallization behavior of 6-APA in a two-feed semi-batch crystallizer under different feed policies, and makes a contrast with the single-feed policy.

2 Experiment

2.1 Materials

6-APA (obtained from the North China Pharmaceutical Co. Ltd.) with 98.0 wt-% purity was regarded as the material to carry out the investigation. Ammonia solution of analytical grade (containing 25 wt-% NH_3) was used. Dilute sulfuric acid of 40 wt-% was prepared by diluting analytical concentrated sulfuric acid of 98 wt-% with deionized water. Deionized water was used to prepare the solutions of 6-APA.

2.2 Experimental setup

The experimental setup was according to the schematic diagram in Fig. 1. It consisted of digital display agitator, 800-mL glass cylindrical crystallizer with double jackets, two sets of feeding devices (peristaltic pump, measuring cylinder and tubes), and on-line observation instruments (FBRM and PVM); a pH meter and a thermometer were used to monitor the process parameters. FBRM and PVM instruments observed the process through the insertion of their probes into the crystallizer. The position of probes in the solution was fixed for each experiment according to the principle explained by Barrett [14]. Two computers were connected to their sensors to respectively record the crystal population and images in the solution during the crystallization process. The system was maintained in required

temperatures by water circulating from a thermostat bath. A rubber plate having several openings was used to cover the crystallizer to avoid any evaporation and fix the probes, feeding tubes, and impeller. Acid and 6-APA solution were dropped into the crystallizer respectively by the peristaltic pump from the measuring cylinder in required speed.

2.3 Experimental procedure

The experimental procedure was as follows: Firstly, an aqueous solution of 6-APA, which can be called the mother liquor required for crystallization, was prepared. Weighed powders for the above solutions and deionized water were added to a separate beaker. Five hundred milliliters of clear solution with a concentration of 40 g/L were prepared by adjusting the pH of the suspension in beaker to 6.5 under continuous stirring. The solutions were filtered with a nano-filtration membrane of $0.45\ \mu\text{m}$ to prevent any impurities that could act as nuclei and hence affect the crystallization process, and then it was ready to perform the reactive crystallization operation as the mother liquor.

In the double-feed semi-batch experiments, the half-volume of total mother liquor was poured into the crystallizer in advance as bottom liquor. At this moment, the FBRM, PVM, and impeller were started simultaneously. The FBRM probe (model M400LF) has a measurement range of $0.25\text{--}1000\ \mu\text{m}$. Sample measurement duration of 5 sec was used for all runs. The PVM probe (model 800 L) was operated with an image update

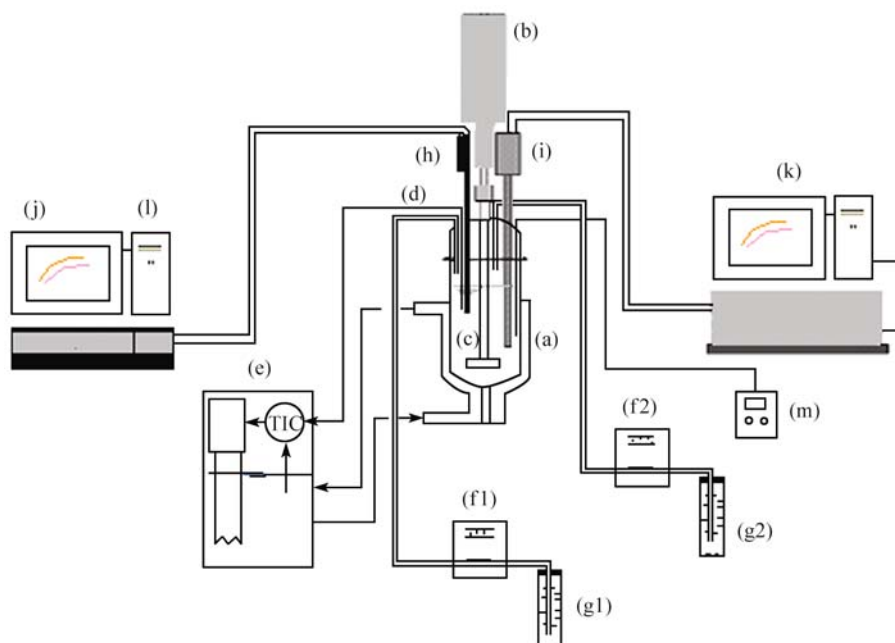


Fig. 1 Experimental set up: (a) 800-mL jacketed glass crystallizer; (b) overhead stirrer; (c) impeller; (d) thermometer; (e) thermostat bath; (f1) peristaltic pump for acid; (f2) peristaltic pump for mother liquor; (g1) measuring cylinder for acid; (g2) measuring cylinder for mother liquor; (h) FBRM probe; (i) PVM probe; (j) FBRM curves; (k) PVM images; (l) computer; (m) pH meter

rate of 2 images per minute. The crystallization process was carried out by feeding acid and the other half-residual mother liquor simultaneously with the settled drop-speeds while stirring in a speed of $250\text{--}270\text{ r}\cdot\text{min}^{-1}$. The drop-speed of the residual mother liquor was fixed at 10 mL/min for all policies, while the feeding speed of H^+ for each process policy was according to Fig. 2.

In traditional single-feed process policy, by contrast, the total volume of mother liquor was poured into the crystallizer and then the acid was introduced into the crystallizer during the crystallization process; the acid feeding would be paused for 20 min when the nucleation occurs. During crystallization, temperature was maintained at 10°C .

At the moment the isoelectric point of 6-APA was reached, which was also the end of reaction, the suspension would be maintained (stop feeding and keep agitation) for 1 h for Ostwald ripening with an impeller speed of $250\text{--}270\text{ r}\cdot\text{min}^{-1}$, and for cooling the system at the same time until it reached 5°C . After that, the 6-APA crystals were quickly isolated by filtration.

3 Results and discussion

3.1 Trend history of particles

Supersaturation is the driving force of a crystallization process, determining the nucleation and growth character of crystals in solution. It was embodied by the variations of

acid feeding policy and pH value in this work. The trends of population and chord length counts in different channel ranges of each policy are drawn in Fig. 3.

Primary heterogeneous nucleation in each experiment occurred as the pH of the mother liquor reached $5.6\text{--}5.8$ and was identified by the sudden increases of population and chord length in $0\text{--}50\text{ }\mu\text{m}$ and total ranges. Since this drastic nucleation greatly consumes supersaturation in the solution, the swiftly increasing population counts reached their peak value after only approximately 10 min. Unlike other policies, the steep curves in experiment E were lower and more inclined, implying a lower nucleation rate. As shown in Fig. 4, the peak value of nucleation rate of single-feeding policy was only 10 number per second ($\#/\text{sec}$), which was much lower than $30\text{--}70\text{ }\#/\text{sec}$ in the four double-feed experiments. The reason was that the total volume of mother liquor existing in the crystallizer which can supply a stronger buffering effect than double-feed policies which only introduce the half of mother liquor in the crystallizer, moderated the drastic accumulation of supersaturation and the burst spontaneous nucleation.

The proceeded curve trends after nucleation were various with acid feeding policies, determined by supersaturation variations of the system in mechanism. A pause of acid-feeding made the crystal population and chord length appear a stagnated period after reaching the first peak value [Fig. 3(E)]. Since supersaturation was generated by feeding acid it had been quickly exhausted in a short period (about 10 min) after pausing and could not

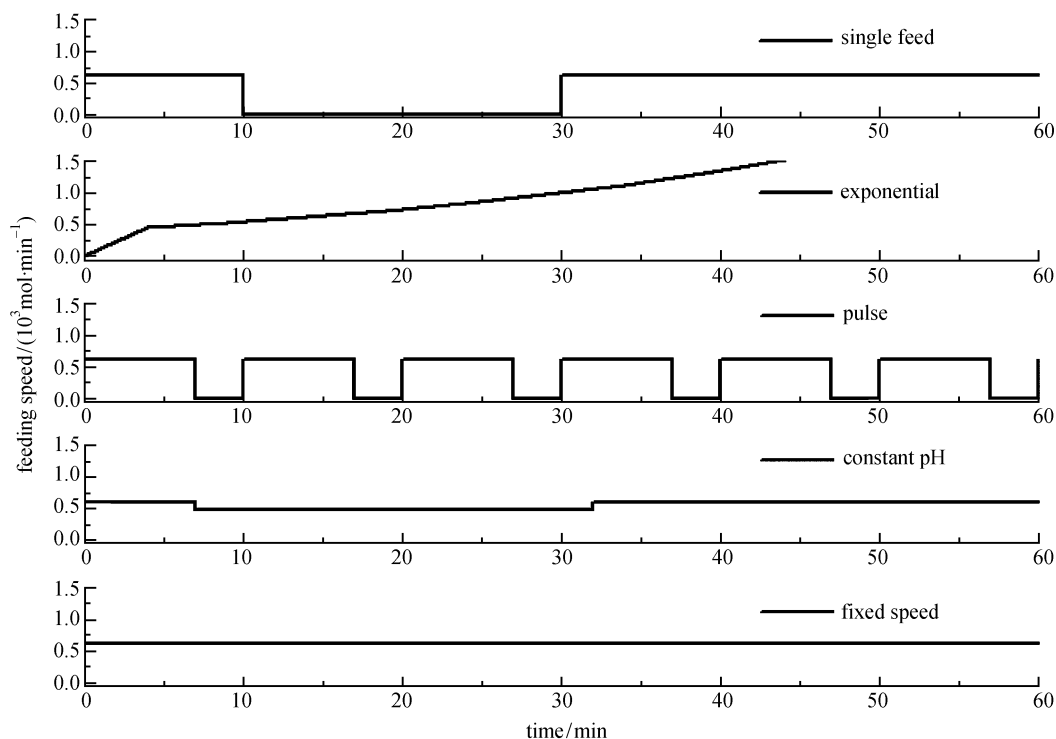


Fig. 2 Acid feeding configuration in different policies

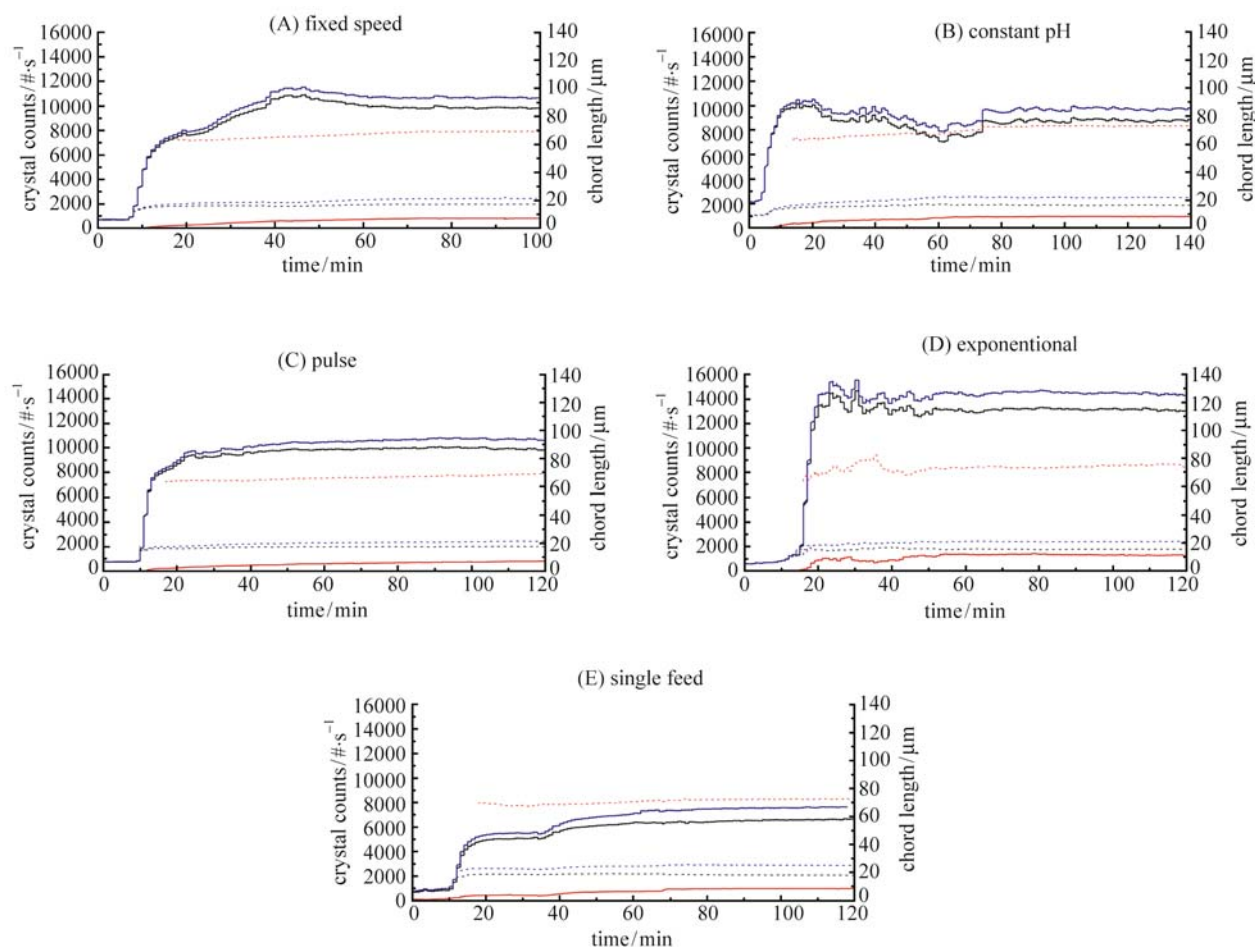


Fig. 3 Trend history of FBRM counts and chord length. Black line, 0–50 μm ; red line, 50–200 μm ; blue line, 0–200 μm . Solid lines represent crystal counts, dashed lines represent chord length

supply any driving force for further nucleation and growth, crystals in solution could only keep their previous conditions. No remarkably breakage was observed in this hold time of 20 min.

In experiment A, a consecutive acid feeding was performed in a fixed speed of 0.6×10^{-3} mol/min after nucleation, which could succeed the energy barrier of nucleation and resulted in both nucleation and growth. So new nuclei were produced after the first primary heterogeneous nucleation [Fig. 3 (A)].

In experiments B and C, there were relatively lower H^+ feeding speeds after nucleation and could only bring a lower supersaturation, which could not conquer the critical energy barrier of nucleation, and just contribute to a slight growth of the present crystals [represented by dashed line in Figs. 3 (B), (C)].

In the Ostwald ripening period after feeding, both the population and the chord length in all ranges approximately kept their previous values; it was a signal that the supersaturation of the system was nearly exhausted over by

a large amount of nucleation and continuous growth during the reaction period and no additional nucleation and growth was occurring. It is necessary to mention here that the yield of all the recrystallization experiments achieved 90 wt-%.

3.2 Habit transformation process

In previous work, the final products of 6-APA with different habits were produced under different operational conditions [6–8].

Observed from the typical PVM images in this work (Fig. 5), the habit of 6-APA was continuously changed during the crystallization process in each policy. At the beginning of nucleation in all experiments, crystals presented a rhombogen [Fig. 5(a)] which showed that the (101) and (020) faces were well developed. Then the (002) face appeared obviously 30 min later. However, the ratio of growth rate between (002) and (101) faces was different in each policy [Fig. 5 (b)]; this difference became more

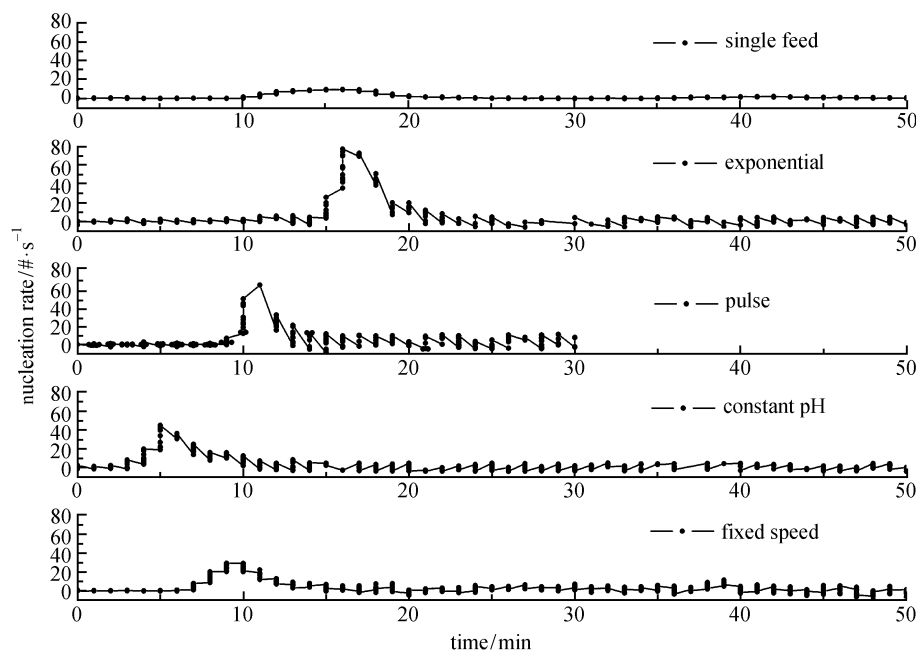


Fig. 4 Nucleation rate in different policies

obvious in the final habit images [Fig. 5 (c)]. Policies with H^+ feeding speeds higher than 0.6×10^{-3} mol/min in feeding period (Experiments of A, D and E) lead to regular hexahedron with equivalent length between the (101) and (002) faces, while others lead to long hexahedron with (002) face significant developed than (101) face. A typical indexed 6-APA crystal is shown in Fig. 6.

In the analysis of the molecule arrangement and attachment energy values of the crystal faces of 6-APA [15], the (002) face shows an amino group or carboxyl group free which could actively absorb the carboxyl group or amino group, and has a attachment energy value of -44.83 kJ/mol. In contrast, the (101) face shows a methyl group with steric hindrance and has an attachment energy value of -26.81 kJ/mol. So the (002) face has the sites of the lowest energy for molecules' orientation which were advantageous for surface integration according to the continuous growth model [15]. Consequently, in higher supersaturated solution, active (002) face had the advantage to absorb 6-APA molecules and hence grew faster than (101) faces (acid feeding for 40 min in Experiments A, D, E), even disappearing (the beginning of nucleation in each experiment).

4 Conclusions

The *in-situ* techniques of FBRM and PVM were successfully used to monitor the statistical particle trends character and morphology development process during reactive crystallization of 6-APA in aqueous solution. From the

analysis above, several conclusions could be drawn:

- 1) Spontaneous nucleation in double-feed crystallizer was much more intense than single-feed policy. Half-volume in initial bottom solution brings in 3–7 times higher in the maximum value of nucleation rate.
- 2) The chord length of 6-APA crystals was almost determined and had little change after the nucleation peak.
- 3) No remarkable growth was observed during the Ostwald ripening period which was performed for 1-hour duration at the end of the 6-APA crystallization process.
- 4) In the reactive crystallization process of 6-APA in semi-feeding crystallizer, agglomeration and breakage were not observed.
- 5) There was a continuous changing of the crystal habit during the crystallization process and has the relationship with the supersaturation, which can lead to the different development of (101) and (002) of the final crystal. At the beginning of nucleation the crystal was rhombus, and the (002) face could not be found at all. The (002) face appeared inchmeal during the subsequent process after nucleation, which means the growth rate of $\langle 100 \rangle$ direction was faster than the $\langle 001 \rangle$ direction.

6) The final crystal habit of 6-APA was determined by the supersaturation after nucleation of the system, which was registered as the acid-adding speed in this paper. If the H^+ adding speed subsequent by the nucleation was faster than 0.6×10^{-3} mol/min, it would lead to the regular hexahedron crystal; on the contrary the speed was lower than 0.6×10^{-3} mol/min conducive to the long hexahedron crystal. These research results will give suggestions to the crystallization process of 6-APA.

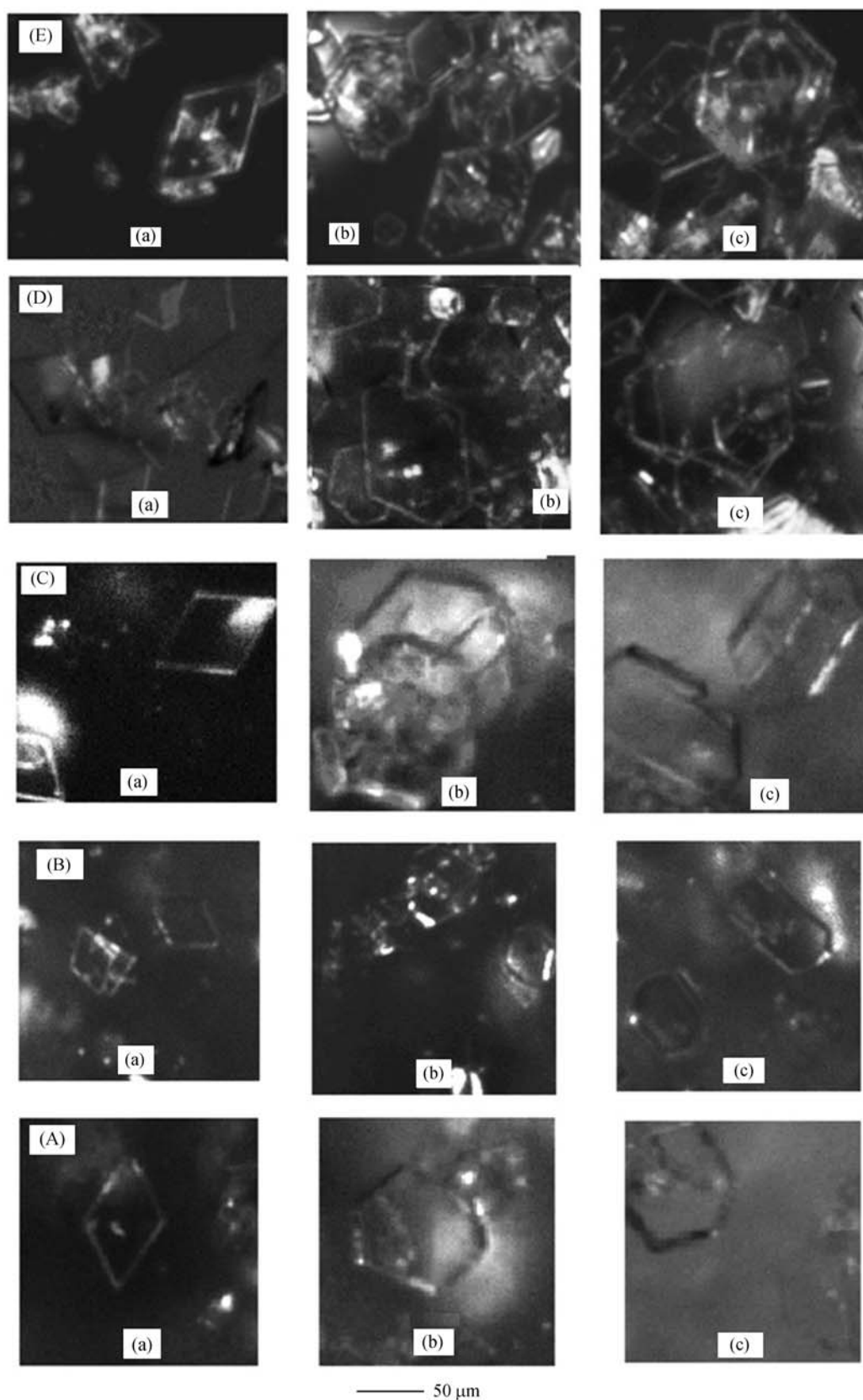


Fig. 5 Habit transformation images; (A) fixed speed policy; (B) constant pH policy; (C) pulse policy; (D) exponential policy; (E) single feed policy. (a) the moment of the nucleation; (b) 30 min after nucleation; (c) the end of crystallization

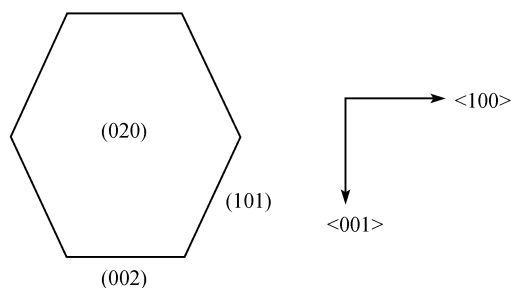


Fig. 6 Typical indexed 6-APA crystal

Acknowledgements The authors thank North China Pharmaceutical Group Corp. (NCPC) for supplying 6-APA and the State Research Center of Industrialization for Crystallization Technology (China) for financial support.

References

1. Vandamme E J. *Biotechnology of Industrial Antibiotics*. New York: Marcel Dekker, 1984
2. Huang H T, Groton C, Seto T A. 6-Aminopenicillanic acid production. US Patent 3212995, 1965
3. Grant N H, Wynnewood, Alburn H E. Method for producing and recovering 6-aminopenicillanic acid. US Patent 3272715, 1966
4. Tavare N S, Jadhav V K. Separation through crystallization and hydrotrophy: the 6-aminopenicillanic acid (6-APA) and phenoxyacetic acid (PAA) system. *Journal of Crystal Growth*, 1999, 199: 1320–1325
5. Rohani S, Horne S, Murthy K. Control of product quality in batch crystallization of pharmaceuticals and fine chemicals. Part 1: Design of the crystallization process and the effect of solvent. *Organic Process Research & Development*, 2005, 9(6): 858–872
6. Mwangi S M, Garside J. Morphology of 6-aminopenicillanic acid crystals and the effect of phenoxyacetic acid. *Journal of Crystal Growth*, 1996, 166(1–4): 1078–1083
7. Gong J B, Wang J K, Wei H Y. Effect of mixed solvents and additives on the habit modification of 6-APA crystals. *Transactions of Tianjin University*, 2005, 11(3): 157–161
8. Gong J B, Wang J K. Effect of supersaturation and temperature on the crystal habits of 6-aminopenicillanic acid. *Chemical Industry and engineering*, 2005, 22(3): 157–160
9. Chew J W, Chow P S, Tan R B H. Automated in-line technique using FBRM to achieve consistent product quality in cooling crystallization. *Crystal Growth & Design*, 2007, 7(8): 1416–1422
10. Shi B, Frederick W J, Rousseau R W. Effects of calcium and other ionic impurities on the primary nucleation of burkeite. *Industrial & Engineering Chemistry Research*, 2003, 42(12): 2861–2869
11. Wang Z Z, Wang J K, Dang L P, Zhang M J. Crystal structures and the solvent-mediated transformation of erythromycin acetone solvate to dihydrate during batch crystallization. *Industrial & Engineering Chemistry Research*, 2007, 46(6): 1851–1858
12. Kougoulos E, Jones A G, Jennings K H, Wood-Kaczmar M. W. Use of focused beam reflectance measurement (FBRM) and process video imaging (PVI) in a modified mixed suspension mixed product removal (MSMPR) cooling crystallizer. *Journal of Crystal Growth*, 2005, 273(3–4): 529–534
13. Shaikh A A, Salman A D, Mcnamara S, Littlewood G, Ramsay F, Hounslow M J. In situ observation of the conversion of sodium carbonate to sodium carbonate monohydrate in aqueous suspension. *Industrial & Engineering Chemistry Research*, 2005, 44(26): 9921–9930
14. Barrett P, Glennon B. In-line FBRM monitoring of particle size in dilute agitated suspensions. *Particle & Particle Systems Characterization*, 1999, 16(5): 207–211
15. Zhang Y. Study on the morphology control of solution crystallization processes for organic compound. Dissertation for the Doctoral Degree. Tianjin: Tianjin University, 2005 (in Chinese)